THERMO-FLUIDIC AND MECHANICAL LOSSES IN A SCROLL EXPANDER FOR AN R134A ORGANIC RANKINE CYCLE

Karthik G. M.[1], Pardeep Garg[2*], Vinod Srinivasan[3] and Pramod Kumar[4]

Indian Institute of Science Bangalore
C V Raman Ave, Bengaluru, Karnataka 560012
[1]karthik.gm1@gmail.com
[2]pardeep_1127@yahoo.com
[3]vinods@mecheng.iisc.ernet.in
[4]pramod_k24@yahoo.com

*Corresponding author

ABSTRACT

In a scroll device, the loss mechanisms can be categorized into two major types; a) thermal fluidic and b) mechanical losses. Further, these losses are found to be strong functions of aspect ratio of a scroll (ratio of scroll diameter and height) and need to be optimized for the best isentropic efficiency. In this paper, a general methodology is developed to optimize the scroll expander geometry for the given operating conditions in any ORC. Detailed results from this methodology are presented for the case study of an ORC with R-134a as a working fluid for different operating conditions. Dependence of individual losses on aspect ratio is understood and presented.

1. INTRODUCTION

Unmatched demand and supply of energy continues to motivate the engineering community to efficiently realize even the marginal potential of low temperature heat sources (~150 °C) which are abundantly available in the form of renewable sources of energy such as geothermal and low concentration solar energy. The scale of these energy sources ranging from a few kW_{th} to MW_{th}, makes scalability a key feature of any chosen energy conversion technology. ORC is a promising technology which is both scalable in the above range and can efficiently generate electricity at low temperatures (Tchanche *et al.*, 2011). In a typical ORC, while pump and heat exchangers are scalable and standardized for a wide range of capacities, choice of expander becomes crucial at power scales below 100 kW_e. At these scales, the conventional turbine type expanders tend to have high rotational speeds (>10^4 rpm) (Fiaschi *et al.*, 2012) and suffer from low isentropic efficiency. Positive displacement devices such as scroll expanders are a possibility in the range of 1 to 100 kW_e (Qui *et al.*, 2011).

Traditionally, scroll has been used as a compressor in refrigeration and air conditioning industry and more recently has started garnering interest as an expander for power generation in micro-scale ORCs. Scientific literature on scroll as an expander can be broadly classified into three major categories, a) experimental testing of scroll in an ORC facility (Saitoh *et al.*, 2007 and Wang *et al.*, 2009), b) numerical simulation using computational fluid dynamic (CFD) (Ooi et al., 2004 and Rogers et al., 1990) and c) analytical modeling including semi-empirical or deterministic models (Quoilin *et al.*, 2010). To predict the overall ORC performance with scroll as an expander, semi-empirical or deterministic models have been developed using the knowledge base generated by above mentioned experimental and computational studies(Lemort *et al.*, 2009 and Guangbin *et al.*, 2010).

A typical feature of these models is to analyze thermal-fluidic losses in detail and assume either a lumped value for calculating the mechanical losses (friction between solid components due to relative motion) (Lemort *et al.*, 2009) or neglecting them (Guangbin *et al*., 2010). However, mechanical losses being an inherent feature of any scroll machine need to be properly examined to design the most efficient geometry, as was done in the case of compressors by Ishii *et al.* (1992) who found that an

optimum combination of scroll height and involute base circle radius results in the maximum efficiency. Such studies are rarely found in the case of scroll expanders. In this paper, a comprehensive study of mechanical and thermal-fluidic losses is carried out for a scroll expander which uses R134a as a working fluid. Furthermore, an optimum combination of geometric parameters is generated for the chosen operating conditions and power capacity of 100 kW_e. Despite being proposed only for applications below 10 kW_e, a 100 kW_e scroll can be physically realized due to low volumetric flow rates observed for the chosen operating conditions.

2. THERMODYNAMIC CYCLE

2.1 ORC details

Figure 1 shows the schematic of the thermodynamic cycle considered in this paper. Low pressure and low temperature liquid at state 1 is pumped to a higher pressure state 2. High pressure fluid at this state is preheated in a regenerator from state 2 to 5 by recovering heat from the expander exhaust wherein the low pressure gas is cooled from state 4 to 6. Remaining heat addition from state 5 to 3 occurs in a heater via a heat transfer fluid (HTF) where it losses heat from state i,HTF to o,HTF. The working fluid is then expanded in a scroll device till state 4. Regenerator outlet on the low pressure side (state 6) is then cooled in an air cooled condenser till state 1 to complete the cycle. Ideal cycle requires the pumping and expansion processes be isentropic and heat transfer processes be isobaric. But real processes are plagued by heat transfer and pressure drop losses, the details of which can found in (Garg *et al.*, 2013 and 2015) .The major assumptions are briefed here.

2.1.1 Cycle assumptions

i. Minimum cycle temperature (T_1) is 45 °C.

ii. To obtain the operating conditions across the scroll, its isentropic efficiency is assumed to be unity which later on is calculated using the scroll model.

iii. Power generation is 100 kW_e.

2.2 Scroll Details

A scroll device consists of a fixed scroll and a moving scroll which translates in a circular orbit. The two scrolls conjugate forming compartments known as chambers. Gas at high temperature and pressure enters at the eye of the scroll and expands as it passes through the various expansion chambers during which it performs work on the moving scroll. Figure 2 shows a typical schematic of the scroll expander. Profile of these scrolls is given by the equation of involute of a circle (equation 1), where r_b is the radius of the base circle.

$$\begin{aligned} x &= r_b\left(\cos\theta + \theta\sin\theta\right) \\ y &= r_b\left(\sin\theta - \theta\cos\theta\right) \end{aligned} \tag{1}$$

2.2.1. Scroll related assumptions

i. The number of scroll turns (wraps) is fixed such that scroll exhaust pressure equals condenser pressure.

ii. The scroll thickness is 5mm which ensures sufficient strength of the scroll walls at the operating pressures analyzed in this paper.

iii. The radial and flank clearance are fixed at 60μm and 80μm respectively

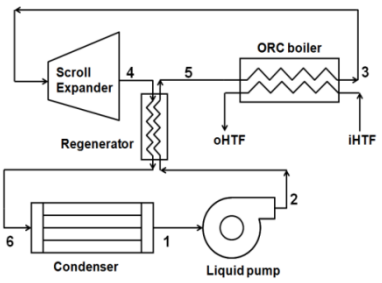

Figure 1: Schematic of an ORC

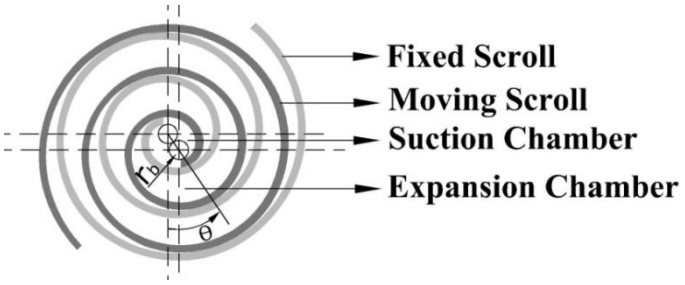

Figure 2: Typical schematic of a scroll expander

3. SCROLL MODELLING

A detailed algorithm for optimizing the scroll geometry is illustrated in Figure 3. For a given scroll inlet temperature, scroll operating conditions are decided by the thermodynamic modeling of the ORC such that they are optimized for the best cycle efficiency. These operating conditions are then fed to the geometric model which generates a number of geometries with different aspect ratios for the given power capacity. These geometries are subsequently evaluated against the best isentropic efficiency by minimizing thermal-fluidic and mechanical losses. These models are herein briefly discussed.

3.1 Geometric Modeling

Based on the required mass flow rate, geometries with different aspect ratios are generated with the various combinations of scroll height (b) and involute base circle radius (r_b). Characteristic parameters of these geometries are also calculated in this model, for example, variation of the chamber area, chamber volume and leakage area, corresponding to flank and radial leakage, with orbiting angle.

3.2 Thermodynamic model

This model calculates the variation of chamber pressure with the orbiting angle which is used to evaluate the loss in isentropic efficiency. Following sub-models are used to calculate the major thermal-fluidic losses.

3.2.1 Supply pressure drop

Ideally, the suction process in a scroll expander is isobaric. However, this is not so due to irreversibilities caused by a pressure drop when the working fluid moves from the suction port to the suction chamber in a finite time. Using the mass flow rate, the corresponding pressure drop can be calculated using equation 2.

$$\dot{m} = A_{su}\rho\sqrt{2(h_{su} - h)} \tag{2}$$

3.2.2 Radial Leakage

Fluid leaking out of the clearances between the moving scroll and the fixed scroll at their top and bottom plane along the spiral length is termed as radial leakage. Modeling of radial leakage is based on Poiseuille's law characterized by laminar flow.

3.2.3 Flank Leakage

Fluid leakage from high to low pressure chamber along the flank walls of the scroll is termed as flank leakage. Leakage amount is calculated using a similar nozzle equation (equation 2) but substituting suction area with flank leakage area.

3.2.4 Heat Transfer

A lumped model is used to calculate the heat transfer losses from the scroll as derived by Lemort *et al.*, 2009 which accounts for the supply and exhaust heat transfer.

3.3 Gas Forces

Chamber pressure variation with orbiting angle already obtained from the thermodynamic model is used to calculate the corresponding gas forces on scroll, namely, F_t (tangential force), F_r (radial force) and M_o (gas moment). Detailed formulations of these forces are given in Ishii *et al.*, 1986.

3.4 Mechanical Modelling

Ishii *et al.* (1986) built a comprehensive scroll compressor mechanical model. In this paper, their model is adapted to a scroll expander and integrated into the ORC model. The various geometrical elements of the scroll are parameterized according to the power capacity of the scroll expander. The following moment equation is derived for the case of an expander at a particular orbiting angle θ of the moving scroll:

$$(I_o + m_s r_o^2 + m_o r_o^2 \sin^2\theta)\ddot{\theta} - m_o r_o^2 \sin\theta \bullet \cos\theta \bullet \dot{\theta}^2 = -N + F_t r_o - \left\{L_Q + L_S + (f_{x1} + f_{x2}) r_o \cos\theta + (f_{y1} + f_{y2}) r_o \sin\theta + (f_{t1} + f_{t2}) r_o\right\} \quad (3)$$

On integrating equation 3 over an entire rotation, while considering steady state with constant angular velocity, and expressing the average of each term over the rotation in terms of work, the following equation is obtained.

$$\underbrace{N\omega}_{A} = \underbrace{F_t r_o \omega}_{B} - \left\{ \underbrace{L_S + L_Q}_{C} + \underbrace{(\mathrm{f}_{t1} + \mathrm{f}_{t2})\,\mathrm{r}_o}_{D} + \underbrace{\frac{1}{2\pi}\int_0^{2\pi} (\mathrm{f}_{x1} + \mathrm{f}_{x2})\,\mathrm{r}_o \cos\theta d\theta + \frac{1}{2\pi}\int_0^{2\pi} (\mathrm{f}_{y1} + \mathrm{f}_{y2})\,\mathrm{r}_o \sin\theta d\theta}_{E} \right\} \omega \quad (4)$$

In equation 4, A is the power output/generator load, B is the work available due to the gas force, C is the loss due to friction in the crank pin and journal bearing, D is the frictional loss in the thrust bearing and E is the frictional loss due to the Oldham coupling. The losses C, D and E have been described below. These frictional losses have been calculated using Coulomb's law of friction and using coefficient of friction μ=0.027 (Ishii *et al.* 1986).

3.4.1 Frictional loss at crank pin and Journal bearing (C)

The crank pin is fixed on the offset crank and is allowed to rotate within the orbiting scroll sleeve bearing, providing the necessary degree of freedom to convert orbiting motion of the scroll to shaft rotation. L_S represents the frictional torque loss at the crank pin. The crankshaft which transfers power from the scroll to the generator passes through a journal bearing. The frictional loss at this bearing is is represented by L_Q.

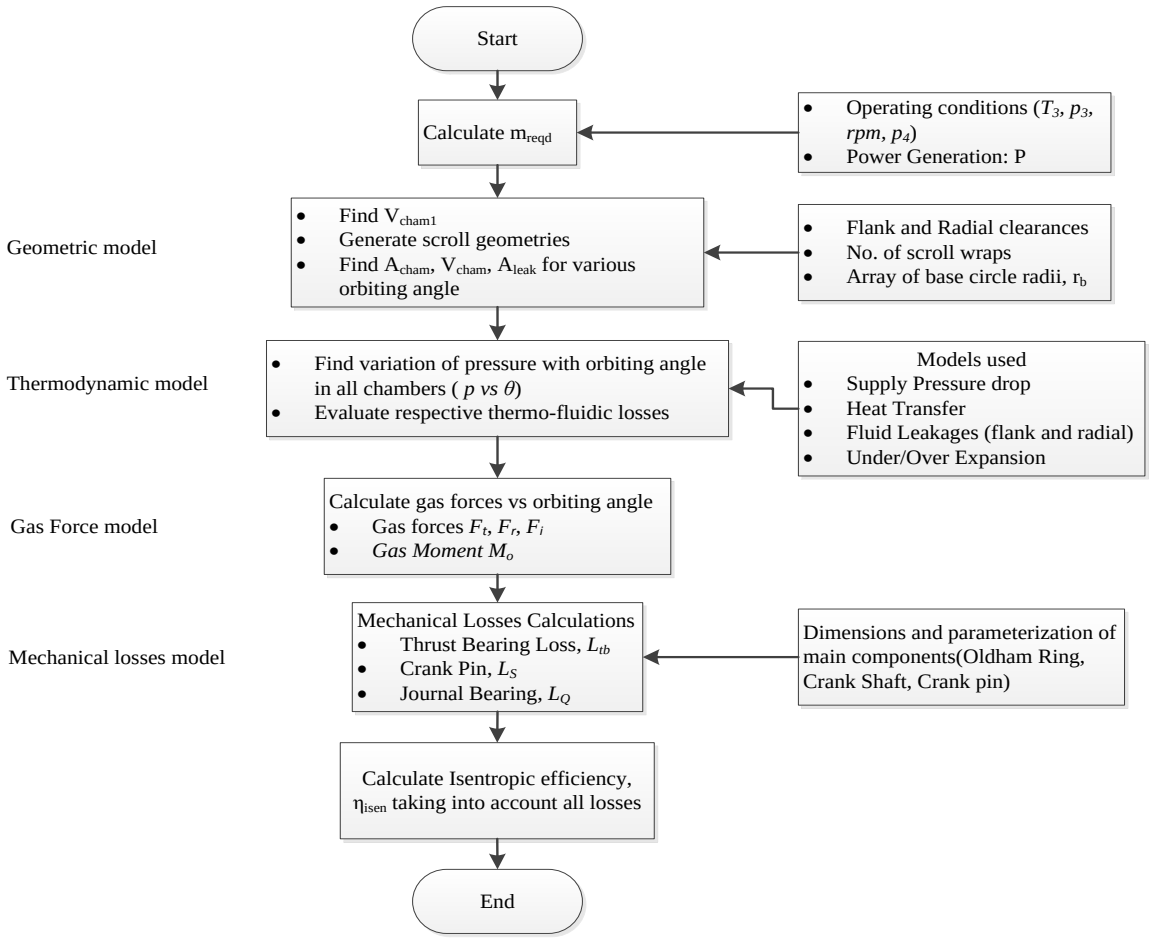

Figure 3: Algorithm followed to optimize the scroll geometry for the given operating conditions of ORC

3.4.2 Thrust Bearing Losses (D)
The resultant thrust force due to gas pressure inside the chamber along with the constraint forces preventing the overturning of the orbiting scroll are supported by the thrust bearing surface. The reaction thrust forces have corresponding frictional forces which represent the thrust bearing losses.

3.4.3 Frictional loss at Oldham coupling (E)
The Oldham coupling slides between the moving scroll and the guide slot on the casing of the scroll machine. The frictional loss due to sliding is very small compared to the other losses.

All calculations were carried out on MATLAB (R-2011b) platform, which was programmed to invoke REFPROP 9.0 database for all thermodynamic property calculations.

4. RESULTS AND DISCUSSIONS

We validated our model against experimental results from Declaye et al. (2013) for an ORC having expander inlet temperature of 105 °C and expander inlet pressure of 12 bar using R245fa as the working fluid. The rotational speed of the scroll was 3000 rpm. Figure 4 shows the isentropic efficiency predicted by our model, which lies within the error limits of Declaye's experimental data. And Figure 5 compares the non-dimensional power generated from the scroll and that predicted by our model.

Scroll geometries studied in this paper are generated for rotational speed of 3000 rpm and various expander inlet temperatures ranging from 100 to 150 °C in the steps of 10 °C. Corresponding expander inlet pressures are chosen at which the cycle efficiencies are maximum and are reported in Table 1. Scroll exhaust pressure is fixed to 12.01 bar corresponding to the saturation pressure of R134a at 45 °C. Various other data like volumetric and pressure expansion ratio across the scroll are also tabulated in Table 1. For a chosen set of operating conditions, a number of scroll geometries are possible with different scroll heights as shown in Figure 6. These geometries need to be optimized for maximum isentropic efficiency. These geometries are then subjected to the evaluation of thermal-fluidic and mechanical losses as described in sections 4.1 and 4.2 respectively. A range of 1 cm to 10 cm was chosen for the height (*b*) of the scroll since optimal geometry with respect to minimum losses was seen within this range for the chosen operating conditions. All the losses are presented in a fractional form as shown below, where X represents the loss model referred to.

$$\eta_{loss,X} = 1 - \frac{\text{scroll work in case loss '}X\text{' is switched on}}{\text{scroll work with all loss switched off}} \tag{5}$$

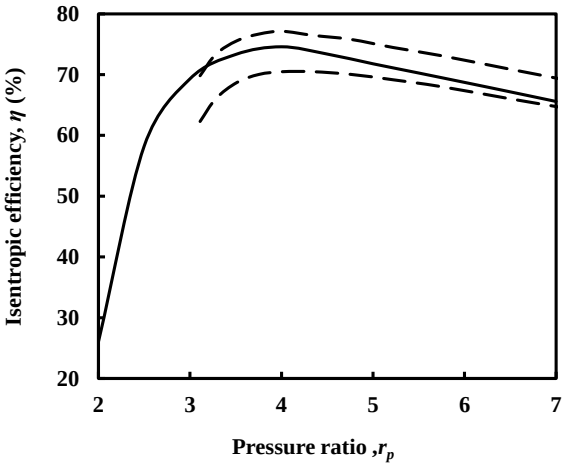

Figure 4: Isentropic efficiency vs pressure ratio Legend: ——Predicted, — — —Experimental Limits (Declaye *et al*., 2013)

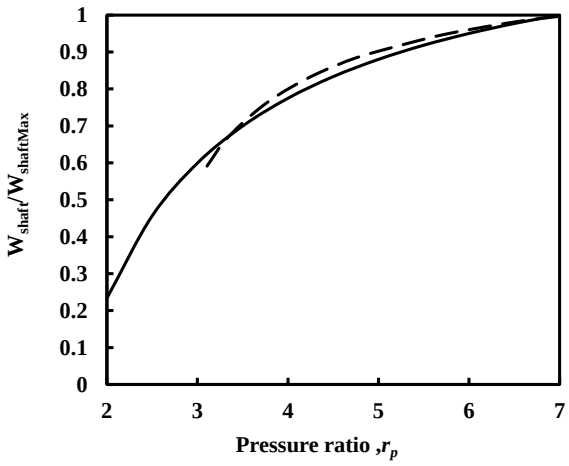

Figure 5: Non dimensional shaft power vs pressure ratio. Legend: ——Predicted, — — — Experiment (Declaye *et al*., 2013)

Table 1: Pressure and volumetric expansion ratio at the various scroll inlet temperatures for an exhaust pressure of 12.1 bar in case of R134a

T_3 (°C)	Optimum R_p	Optimum $\eta_{cycle(\%)}$	Optimum R_v	p_3 (bar)
100	2.80	10.17	3.17	33.61
110	2.97	11.11	3.30	35.76
120	3.31	12.31	3.66	39.74
130	3.63	13.50	3.99	43.61
140	4.01	14.68	4.38	48.15
150	4.40	15.85	4.78	52.90

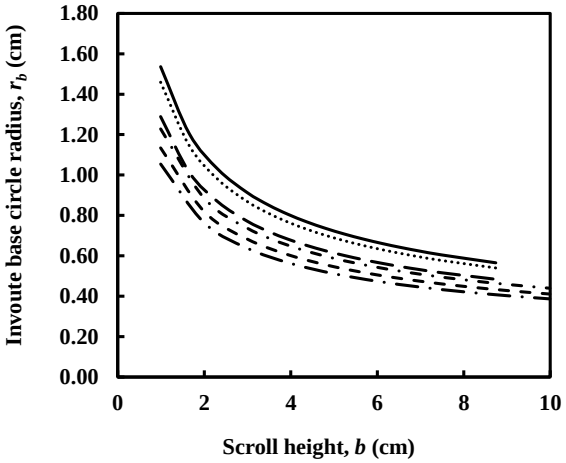

Figure 6: Scroll base circle radius vs scroll height. Legend: ——T_3=100 °C,····· T_3=110 °C, — — — T_3=120 °C, – · – · –T_3=130 °C, – – – T_3=140 °C, —— · —— · ——T_3=150 °C

4.1. Thermal-fluidic losses

Fractional loss due to supply pressure drop against the scroll height is plotted in Figure 7. As scroll height increases, gas inlet area to the scroll decreases which results in higher supply pressure drop and hence the losses associated with it. At constant scroll inlet temperature, these losses are found to be roughly linear with scroll height. However, increase in scroll inlet temperature (T_3) decreases the supply pressure drop losses due to lower mass flow rates required to generate the same power output.

For the given scroll operating conditions, there exists a unique scroll geometry for which heat transfer losses are minimized as observed in Figure 7. Further, scroll geometry resulting in minimum heat transfer losses corresponds to minimum scroll surface area. As expected, heat transfer losses increase with scroll inlet temperature.

The loss due to flank leakage, Figure 8, is noted to increase with height of the scroll expander which can be directly attributed to the increase in leakage area along the flank of scroll wall. Also the leakage losses increase with supply temperature due to a corresponding increase in supply pressure. There is no distinct optimum scroll height observed for minimization of flank leakage losses contrary to the heat transfer losses.

Losses due to radial leakage are directly proportional to the spiral length of the scroll as can be seen in Figure 8, which in turn decreases with increase in scroll height. For higher scroll inlet temperatures, higher radial leakage losses are noted which is again attributed to higher scroll inlet pressure

4.2 Mechanical losses

As seen in Figure 9, fractional loss due to friction in the thrust bearing decreases with increase in height of scroll due to a corresponding decrease in the thrust bearing area of the scroll. Also a minima

is seen after which the losses rise marginally, indicating existence of an optimal choice of height (b) of the scroll. Its behavior is independent of the supply temperature.

The losses in the crank pin and journal bearing show minima at a particular height. Furthermore, this optimal height is seen to decrease with increase in supply temperature, which could be attributed to a corresponding increase in supply pressure.

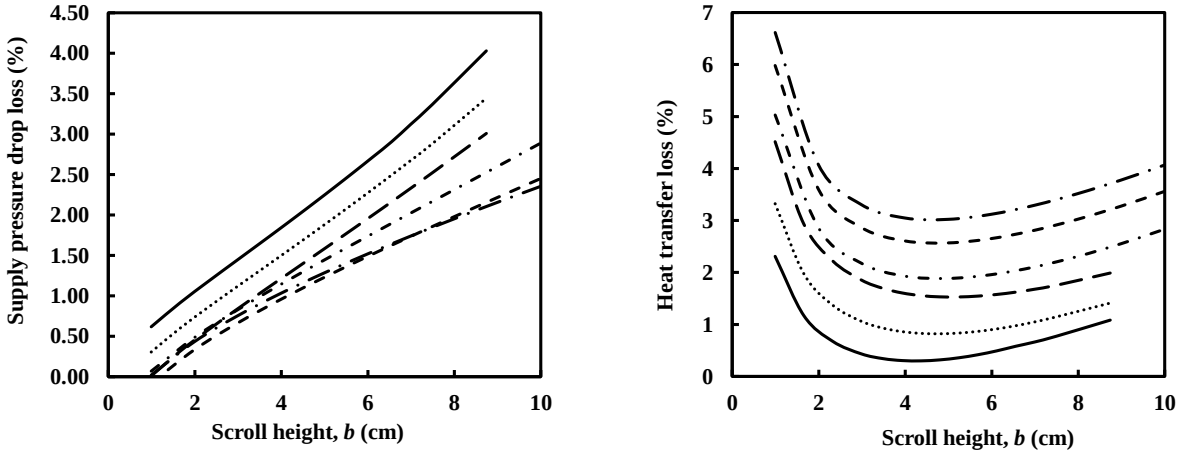

Figure 7: Variation of Supply Pressure drop losses and Heat transfer losses with scroll height. Legend: ——T_3=100 °C, ····· T_3=110 °C, — — — T_3=120 °C, – · – · –T_3=130 °C, – – – T_3=140 °C, —·—·—T_3=150 °C

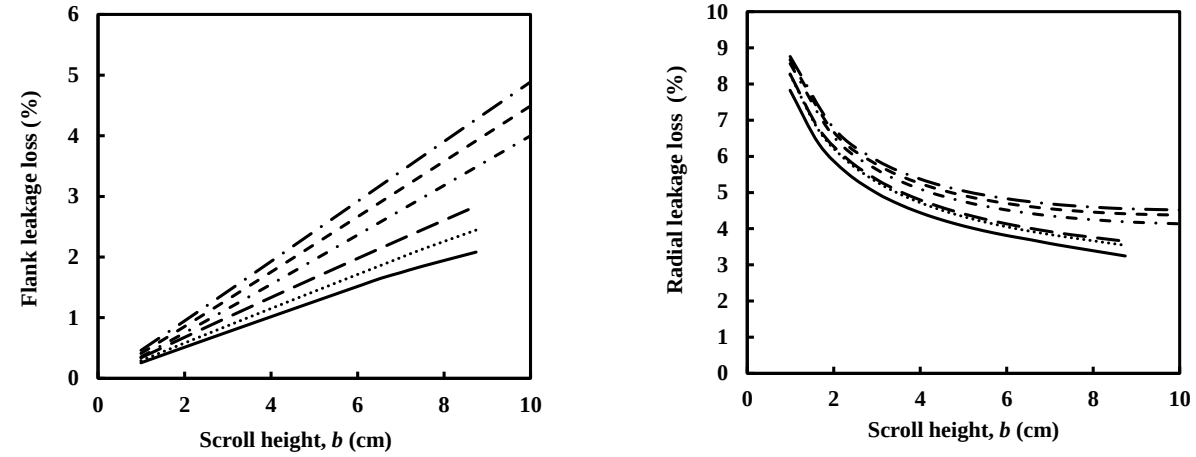

Figure 8: Variation of Flank leakage loss and Radial leakage loss with scroll height. Legend: ——T_3=100 °C, ····· T_3=110 °C, — — — T_3=120 °C, – · – · –T_3=130 °C, – – – T_3=140 °C, —·—·—T_3=150 °C

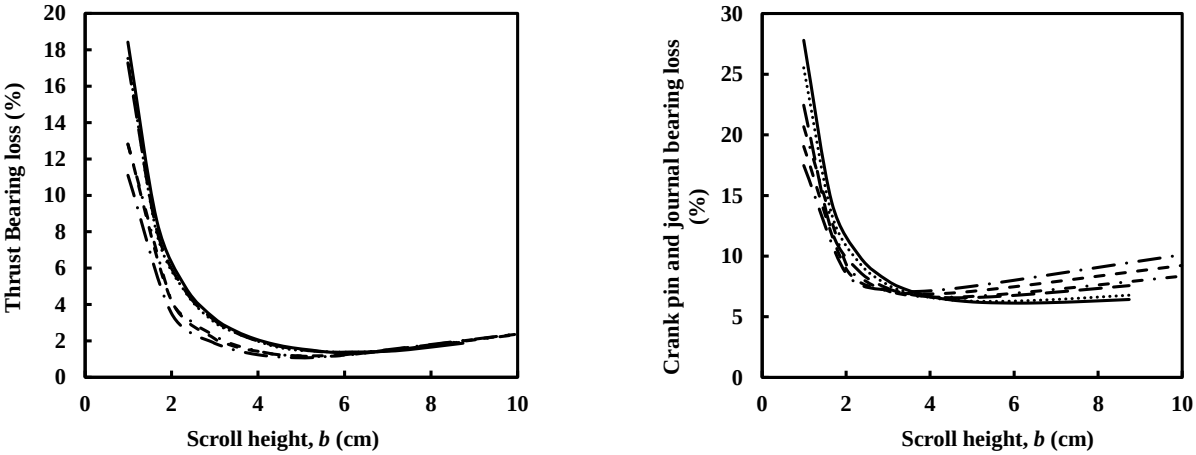

Figure 9: Variation of Thrust bearing losses and Crank pin and Journal bearing loss with scroll height. Legend: —— T_3=100 °C, ····· T_3=110 °C, — — — T_3=120 °C, – · – · – T_3=130 °C, – – – T_3=140 °C, —·—·— T_3=150 °C

4.3 Overall Losses

The distribution of the various losses can be seen in Figure 10 for the case of T_3 = 120 ºC.

Figure 11 shows the overall isentropic efficiency of the scroll expander as a function of scroll height. This graph includes the effect of all the losses discussed above. As can be seen there exists an optimal height at which maximum isentropic efficiency of the scroll expander exists. Also this optimal height is a function of the expander inlet temperature and monotonically decreases with increase in the expander inlet temperature as can be seen in Figure 12. The following equation can be used to obtain the optimal height as a function of temperature.

$$b_{opt} = -0.000387T_3 + 0.2061 \tag{4}$$

Also for the case of constant expander inlet pressure p_3 of 33.16 bar and varying expander inlet temperature T_3, the optimal height is seen to be almost constant indicating the influence of expander inlet pressure on the optimal geometry of the scroll expander.

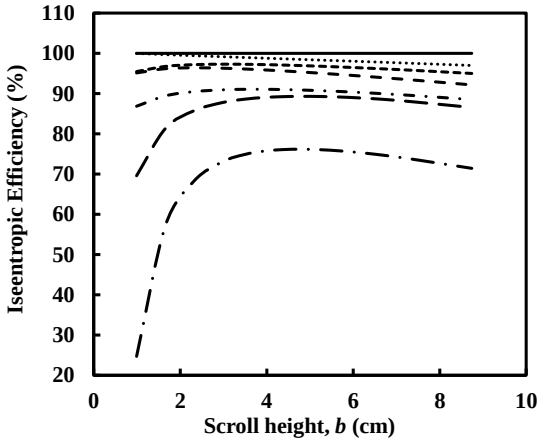

Figure 10: Variation of overall Isentropic efficiency with scroll height for scroll inlet temperature of 120 ºC. Legend: —— Ideal, ····· +Supply Pressure Drop, ------+ Heat Transfer Loss, − − −+ Flank Leakage, − · − · − +Radial Leakage, ———— Thrust Bearing Losses, —— · —— · —— Journal Bearing Losses

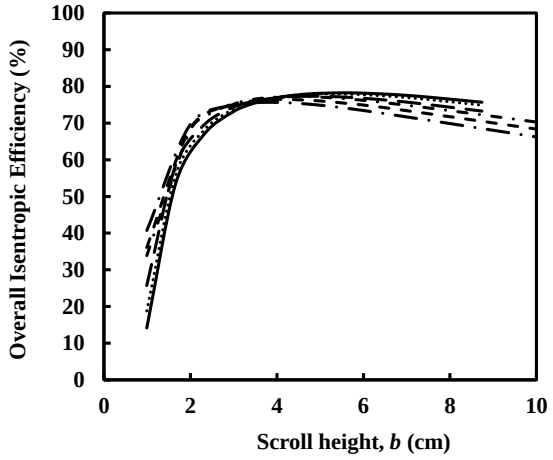

Figure 11: Variation of overall Isentropic efficiency with scroll height. Legend: ——T_3=100 °C,····· T_3=110 °C, — — —T_3=120 °C, − · − · −T_3=130 °C, − − − T_3=140 °C, —— · —— · ——T_3=150 °C

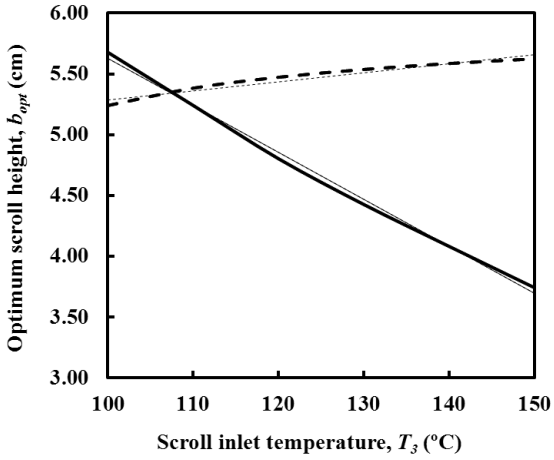

Figure 12: Optimum Scroll Height vs Supply Temperature. Legend: ——Optimum P_3 corresponding to T_3, − − −p_3=33.16 bar

5. CONCLUSIONS

In this paper, a procedure to optimize the scroll geometry for maximum isentropic efficiency for the given operating conditions and choice of working fluid in an ORC is presented. Selection of optimum geometry is based on minimizing the major losses in a scroll device namely, thermal-fluidic and mechanical losses which strongly depend upon the aspect ratio. Key findings from the case study of R134a ORC are as follows:

i. Break up of these losses predicts mechanical losses to be of significant importance and hence, mechanical losses need to be properly accounted for.

ii. Lumped models for mechanical losses may miss the optimum scroll geometry as the mechanical losses are found to be strong functions of scroll aspect ratios.

iii. Keeping the pressures across the scroll identical, the optimum scroll height remains fairly constant with increase in scroll inlet temperature. On the other hand, if pressures in the scroll increase, optimum height decreases indicating higher aspect ratios.

Further, the tool developed herein can be implemented for the various working fluids and for different power scales to draw a comparison among them on the basis of optimum isentropic efficiency, scroll dimensions and cost.

NOMENCLATURE

A_{su}	suction area	m^2
b	scroll height	m
b_{opt}	optimum scroll height	m
F_i	axial force	N
F_r	radial force	N
F_t	tangential force	N
f_{x1}, f_{x2}, f_{y1}, f_{y2}	frictional force at Oldham ring	N
h	enthalpy	kJ/kg
I_o	crank shaft moment of inertia	kgm^2
L_Q	frictional torque at crank journal	Nm
L_S	frictional torque at crank pin	Nm
m	mass flow rate	kg/s
M_o	gas moment	Nm
m_s	mass of orbiting scroll	kg
N	generator load	W
p	pressure	N/m^2
r_b	base circle radius	m
r_o	orbiting radius	m
R_p	Pressure ratio	(-)
R_v	Expansion ratio	(-)
T	temperature	K
V	volume	m^3
θ	scroll orbiting angle	rad
ω	angular speed	rad/s
ρ	density	kg/m^3

REFERENCES

Declaye, S., Quoilin, S., Guillaume, L., Lemort, V., 2013, Experimental study on an open-drive scroll expander integrated into an ORC (Organic Rankine Cycle) system with R245fa as working fluid. *Energy*, vol. 55, p: 173-183.

Fiaschi, D., Manfrida, G., Maraschiello, F., 2012, Thermo-fluid dynamics preliminary design of turbo-expanders for ORC cycles, *Applied Energy*, vol. 97: p. 601–608.

Garg, P., Kumar, P., Srinivasan, K., Dutta, P., 2013, Evaluation of carbon dioxide blends with isopentane and propane as working fluids for organic Rankine cycles, *Applied Thermal Engineering*, vol. 52, p: 439-448

Garg, P., Kumar, P., Srinivasan, K., 2015, A trade-off between maxima in efficiency and specific work output of super- and trans-critical CO2 Brayton cycles, *The Journal of Supercritical Fluids*, vol. 98, p: 119–126

Guangbin, L., Yuanyang, Z., Liansheng, L., Pengcheng, S., 2010, Simulation and experiment research on wide ranging working process of scroll expander driven by compressed air, *Applied Thermal Engineering*, vol. 30, no. 14: p. 2073-2079.

Lemort, V., Quoilin, S., Cuevas, C., Lebrun, J., 2009, Testing and modeling a scroll expander integrated into an Organic Rankine Cycle, *Applied Thermal Engineering*, vol. 29, no. 14: p. 3094-3102.

Ooi, K. T., Zhu, J., 2004, Convective heat transfer in a scroll compressor chamber: a 2-D simulation, *International Journal of Thermal Sciences*, vol. 43, no. 7: p. 677-688.

Tchanche, B. F., et al, 2011, Low-grade heat conversion into power using organic Rankine cycles – A review of various applications, *Renewable and Sustainable Energy Reviews*, vol. 15, no. 8: p. 3963–3979.

Quoilin, S., Lemort, V., Lebrun, J., 2010, Experimental study and modeling of an Organic Rankine Cycle using scroll expander, *Applied energy*, vol. 87, no. 4: p. 1260-1268.

Saitoh, T., Yamada, N., Wakashima, S. I., 2007, Solar Rankine cycle system using scroll expander, *Journal of Environment and Engineering*,vol. 2, no. 4: p. 708-719.

Wang, H., Peterson, R. B., Herron, T., 2009, Experimental performance of a compliant scroll expander for an organic Rankine cycle, *Proceedings of the Institution of Mechanical Engineers, Part A: Journal of Power and Energy*, vol. 223, no. 7: p. 863-872.

Ishii, N., Fuhushima, M., Sano, K., Sawai, K., 1986, A study on dynamic behavior of a scroll compressor, *International Compressor Engineering Conference*, Paper 578.

Ishii, N., Yamamoto, S., Muramatsu, S., Yamamura, M., Takahashi, M., 1992, Optimum combination of parameters for high mechanical efficiency of a scroll compressor, *International Compressor Engineering Conference*, Paper 798.

Morishita, E., Sugihara, M., Inaba, T., Nakamura, T., 1984, Scroll Compressor Analytical Model, *International Compressor Engineering Conference*, Paper 495.

Rogers, R. J., Wagner, R. C., 1990, Scroll compressor flow modeling: experimental and computational investigation, *International Compressor Engineering Conference*, Paper 707.

ACKNOWLEDGEMENT

This research is based upon work supported by the Solar Energy Research Institute for India and the U.S. (SERIIUS) funded jointly by the U.S. Department of Energy subcontract DE AC36-08G028308 (Office of Science, Office of Basic Energy Sciences, and Energy Efficiency and Renewable Energy, Solar Energy Technology Program, with support from the Office of International Affairs) and the Government of India subcontract IUSSTF/JCERDC-SERIIUS/2012 dated 22nd Nov. 2012.